Supporting Information

Exciton-Phonon coupling in quasi-two-dimensional Ruddlesden-Popper perovskites: Impact of mixed-phase structure

Sushovan Sarkar [1,2], Nagendra S Kamath [1,2], Koushik Gayen [1,2], and Suman Kalyan Pal [1,2]

[1]School of Physical Sciences, Indian Institute of Technology Mandi, Kamand, Mandi-175005, Himachal Pradesh, India

[2]Advanced Materials Research Centre, Indian Institute of Technology Mandi, Kamand, Mandi-175005, Himachal Pradesh, India

AUTHOR INFORMATION

Corresponding Author

*E-mail: suman@iitmandi.ac.in; Phone: +91 1905 267040

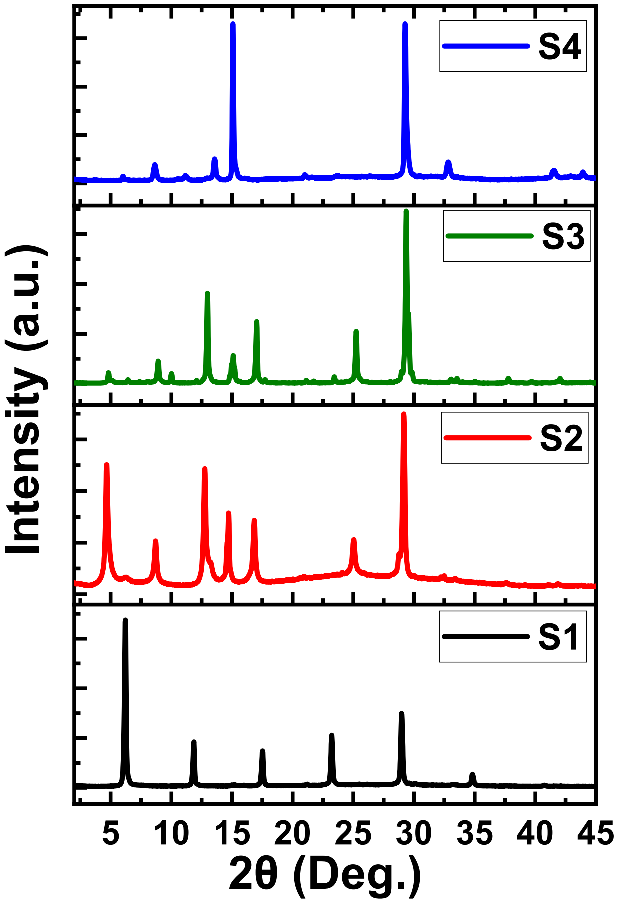

Fig. S1 X-ray diffraction (XRD) patterns of $(TEA)_2(MA)_{n-1}Pb_nI_{3n+1}$ (n=1-4) perovskite films.

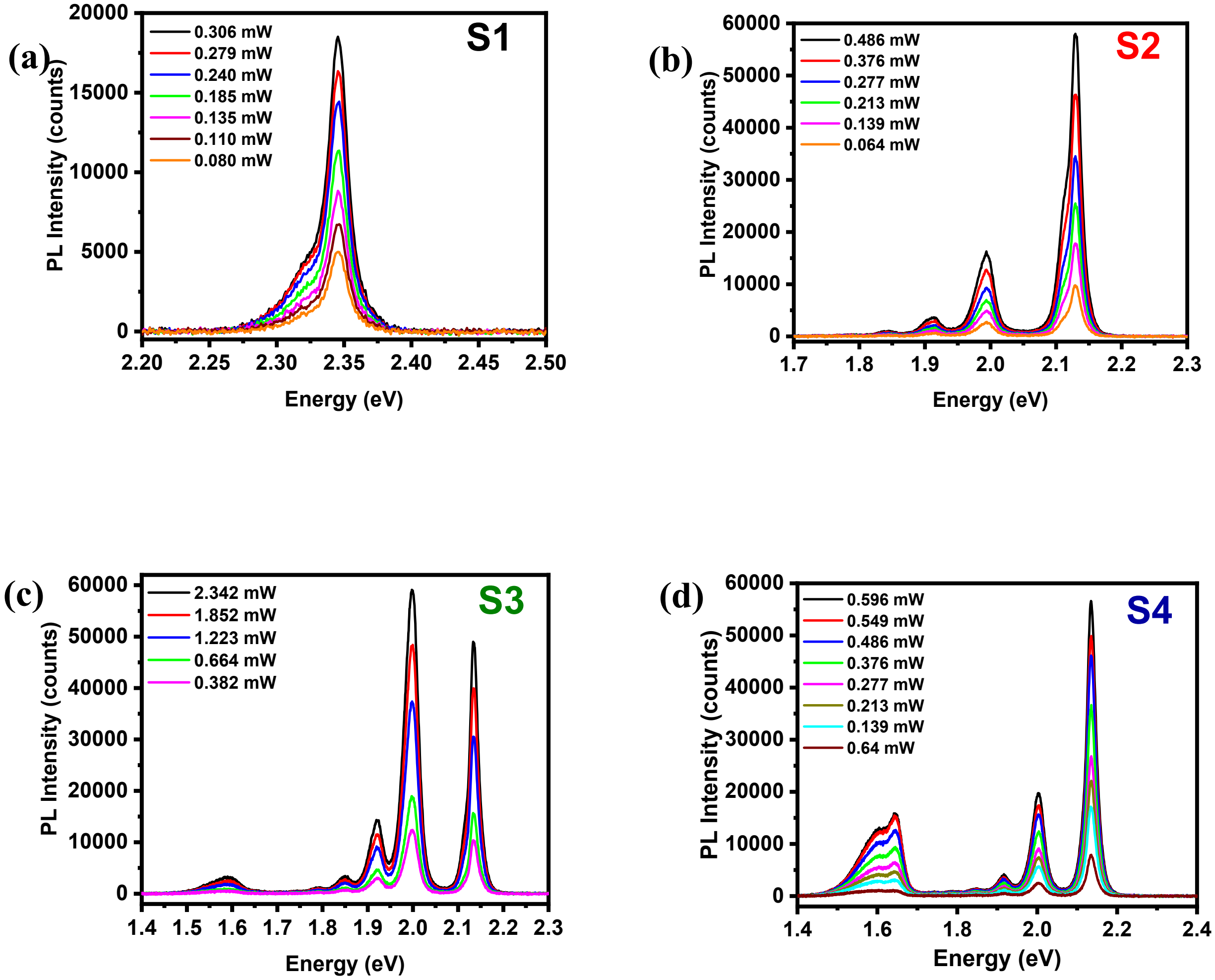

Fig. S2 Excitation power dependent photoluminescence (PL) spectra of $(TEA)_2(MA)_{n-1}Pb_nI_{3n+1}$ (n=1-4) films (S1-4) measured at 83 K.

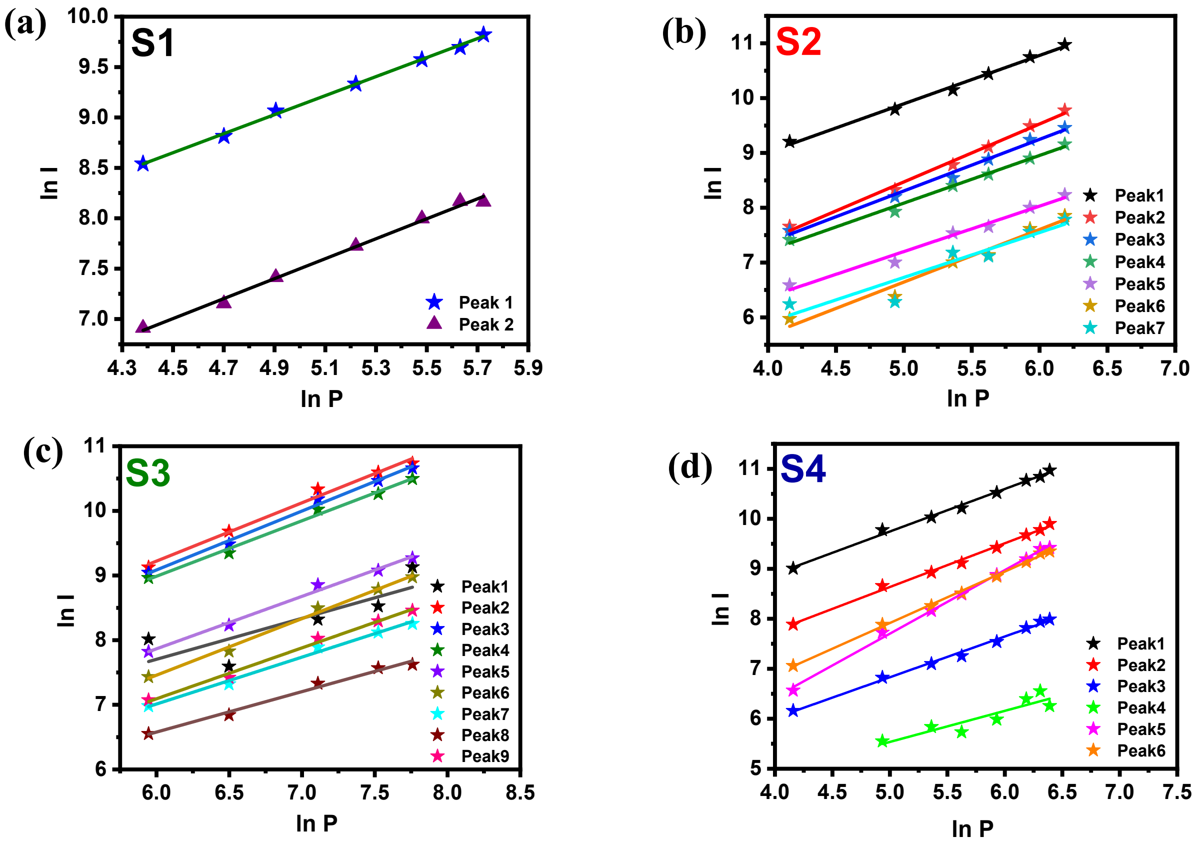

Fig. S3 Variation of maximum PL intensity (I) of each peak as a function of excitation power (P) for S1-4. The solid lines represent straight line fitting of lnI vs lnP.

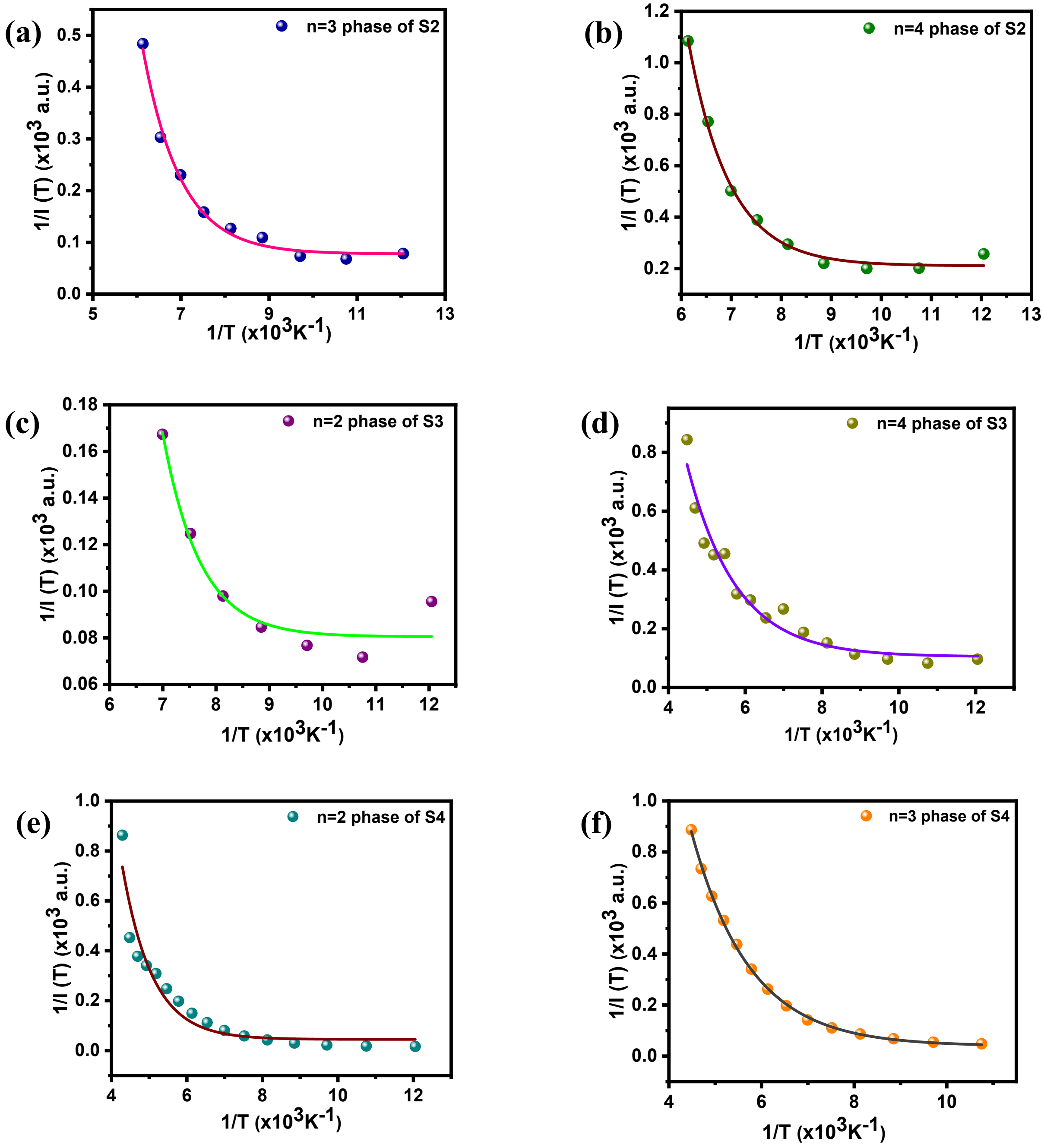

Fig. S4 Experimentally obtained inverse of integrated PL intensity [1/I(T)] vs inverse of temperature (1/T) plots fitted (solid line) using eqn (1) for different phases of samples S2, S3 and S4.

Table S1 Values of exciton binding energy (meV) in different 2D phases obtained by fitting 1/I(T) vs 1/T plots using eqn (1).

Phase / Sample	n=1	n=2	n=3	n=4
S1	230 ± 16			
S2		137 ± 12	100 ± 9	104 ± 8
S3		122 ± 37	109 ± 8	67 ± 9
S4		108 ± 19	68 ± 1	64 ±5

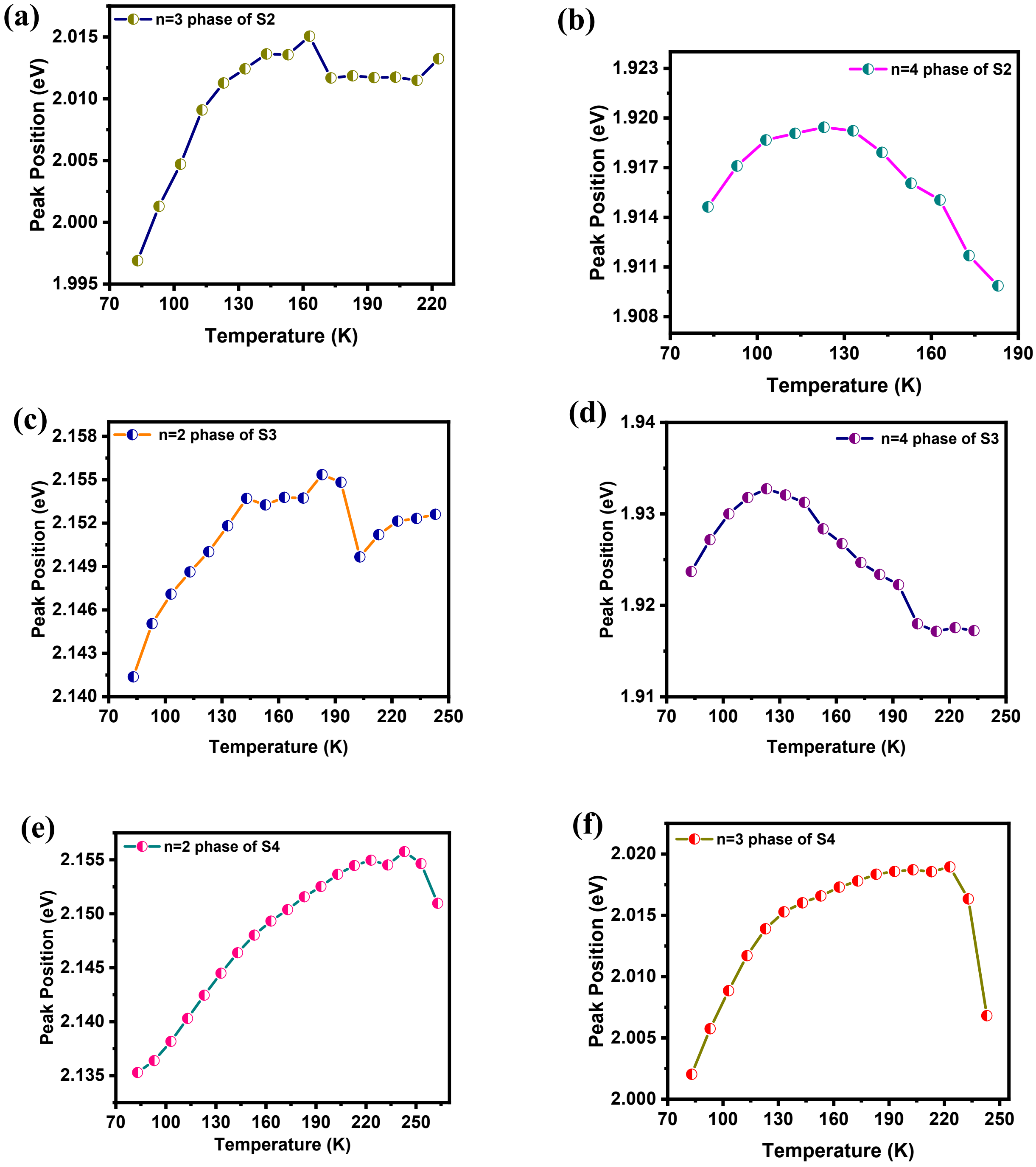

Fig. S5 Evolution of PL peak positions as a function of temperature for different phases of samples S2, S3 and S4.

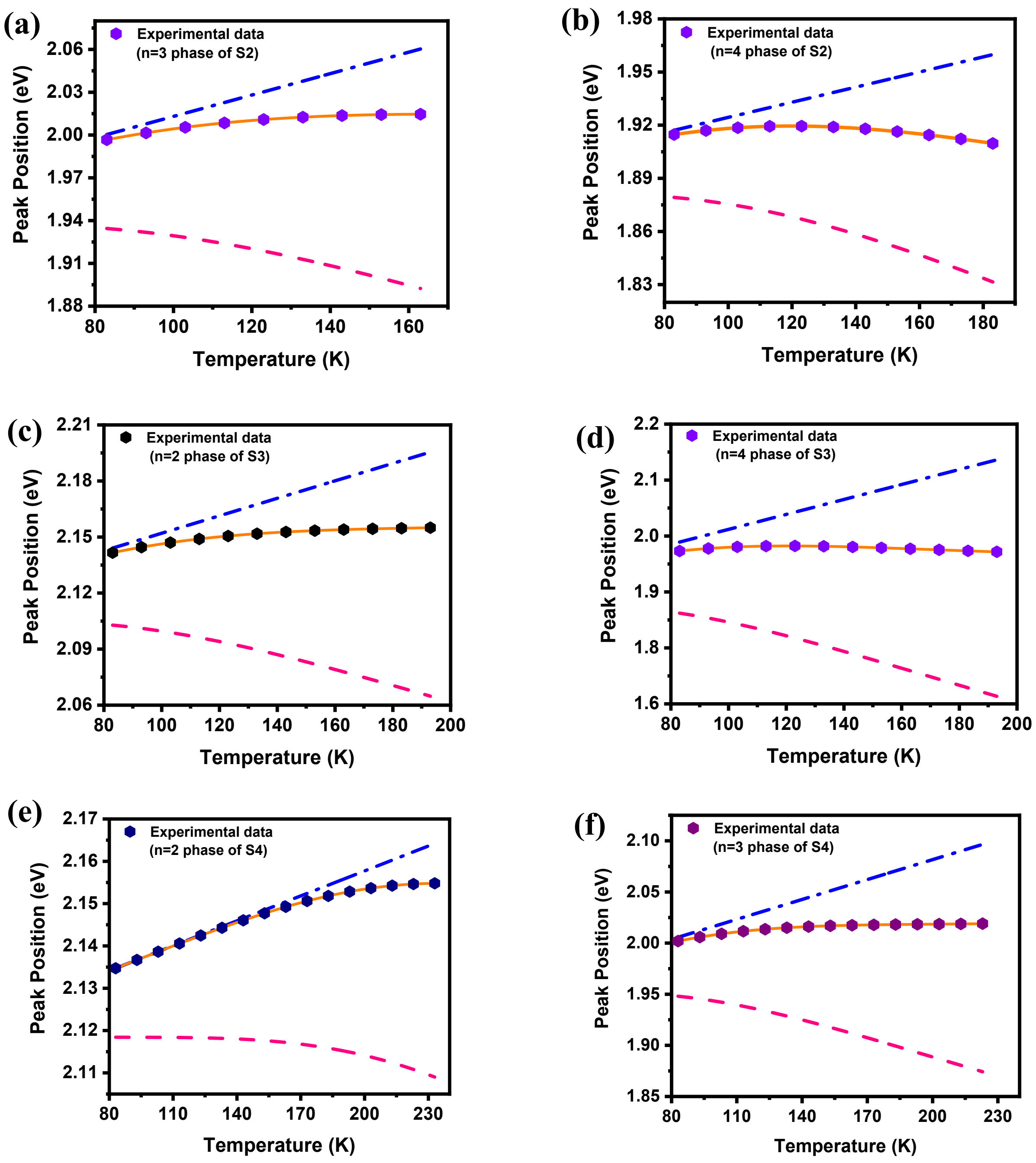

Fig. S6 Temperature-dependent PL peak positions of different phases of sample S2, S3 and S4 fitted with eqn (3) (solid lines). The dashed-dotted (blue) and dashed (pink) lines show contributions of thermal expansion and electron-phonon interaction, respectively.

Table S2 The parameters estimated from fitting of experimental data shown in Fig. S6 using eqn (3).

Sample	**Phase**	**E_0 (eV)**	**A_{TE} (meV/K)**	**A_{EP} (meV)**	**$\hbar\omega$ (meV)**
S2	**n=2**	2.073 ± 0.001	0.88 ± 0.03	-176.94 ± 4.96	21.56 ± 1.05
	n=3	1.94 ± 0.02	0.75 ± 0.01	-314.78 ± 36.67	36.77 ± 2.13
	n=4	1.88 ± 0.02	0.43 ± 0.02	-309 ± 39	39.52 ± 8.25
S3	**n=2**	2.11 ± 0.01	0.47 ± 0.17	-166.03 ± 26.94	34.91 ± 6.84
	n=3	1.85 ± 0.01	1.78 ± 0.21	-578.17 ± 41.57	29.72 ± 1.10
	n=4	1.83 ± 0.02	1.34 ± 0.26	-478 ± 57	29.20 ± 1.38
S4	**n=2**	2.118 ± 0.001	0.197 ± 0.004	-549.15 ± 35.15	95.33 ± 7.71
	n=3	1.952 ± 0.003	0.65 ± 0.04	-232.18 ± 10.42	34.30 ± 0.93
	n=4	1.80 ± 0.02	1.53 ± 0.25	-476 ± 60	26.90 ± 0.83

Table S3 Calculated values of the fraction of free charge carriers over the total excitation density (x) for the main peaks of all the samples.

Sample	**Phase**	**x**	
		High temperature	**83 K**
S1	**n=1**	0.19 (298K)	7.55 x 10^{-7}
S2	**n=2**	0.34 (243K)	0.0003
S3	**n=3**	0.31 (243K)	0.0011
S4	**n=4**	0.80 (223K)	0.05

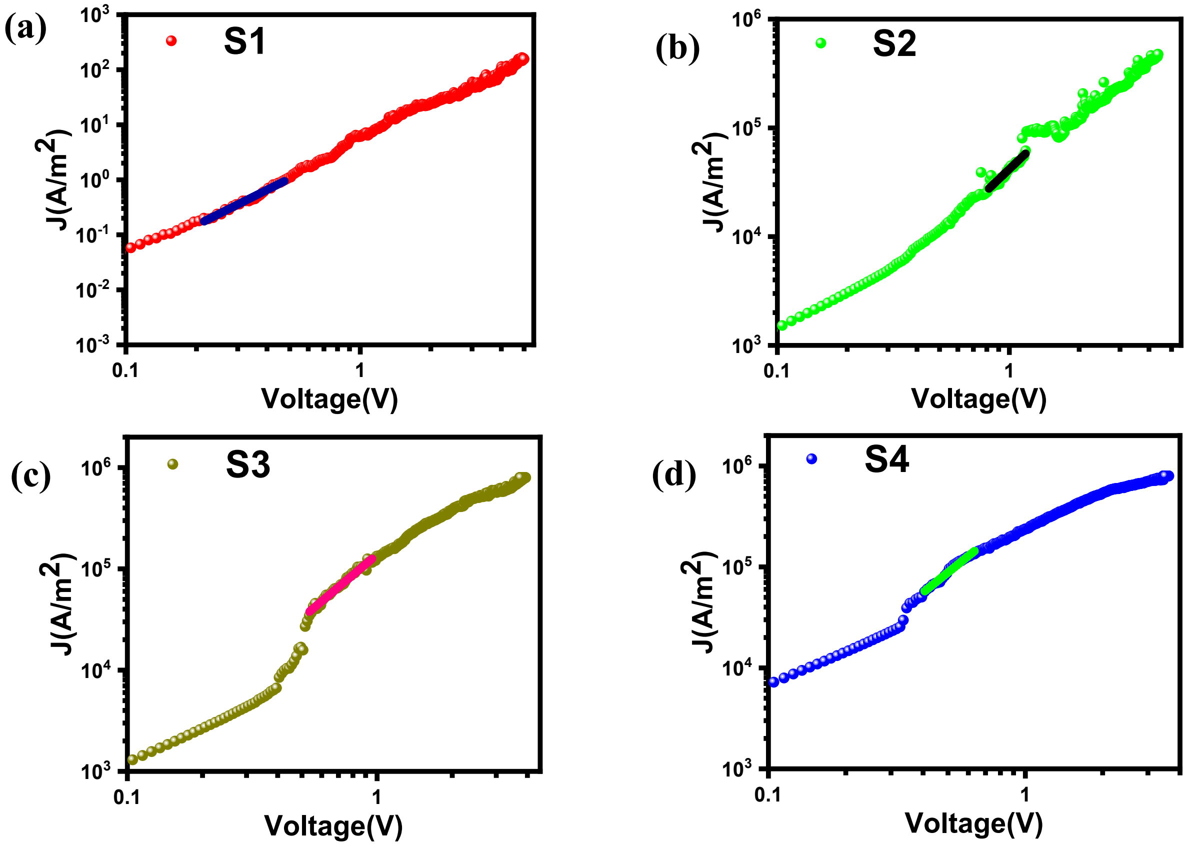

Fig. S7 J-V curves in a log-log scale for devices fabricated from samples S1–S4. The solid lines represent the fitting of the SCLC region using eqn (5).

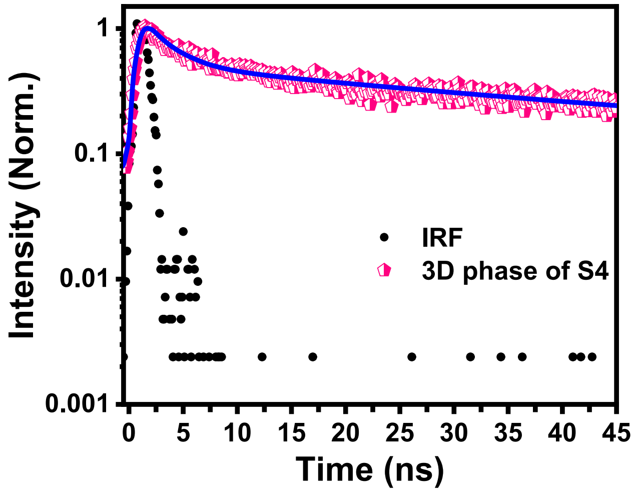

Fig. S8 TRPL curves of the 3D phase of sample S4 at an excitation wavelength of 400 nm. The solid line is the fitted curve using eqn (6).

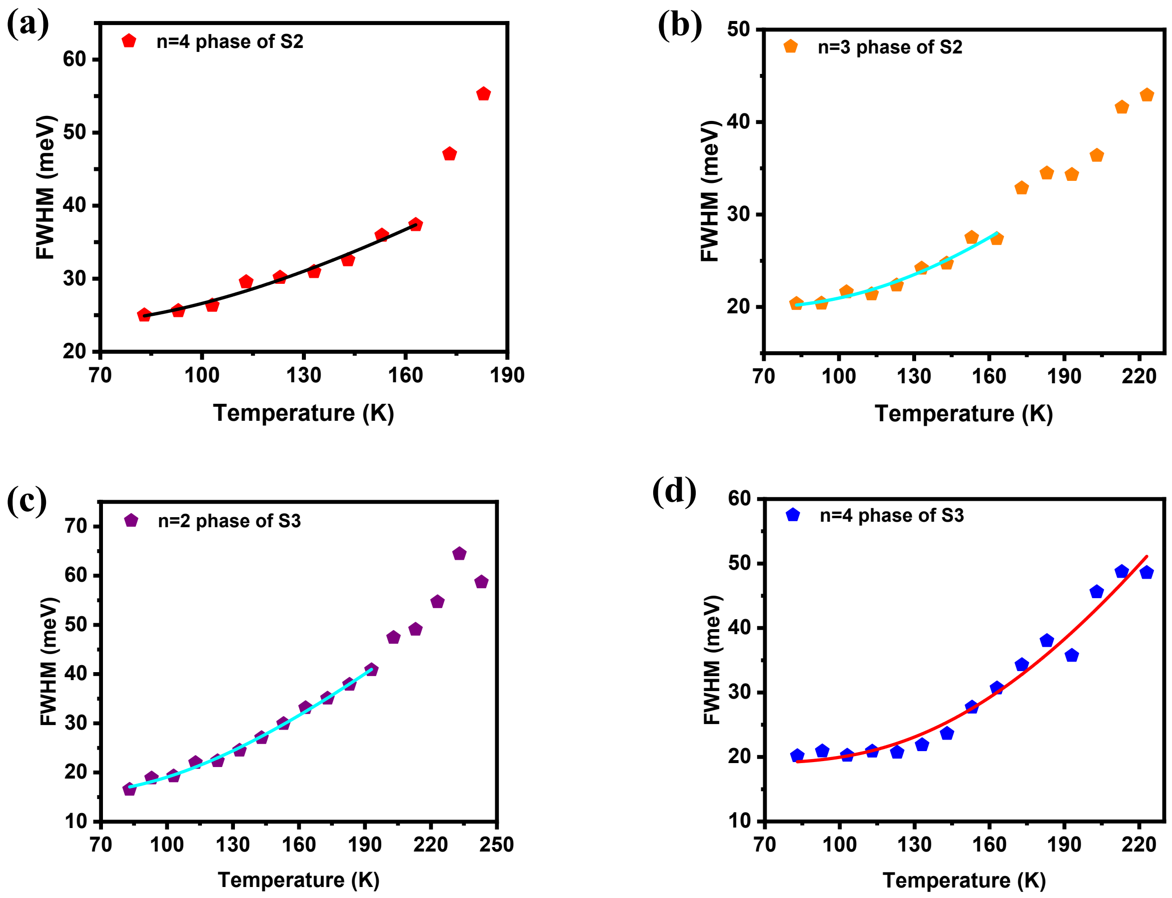

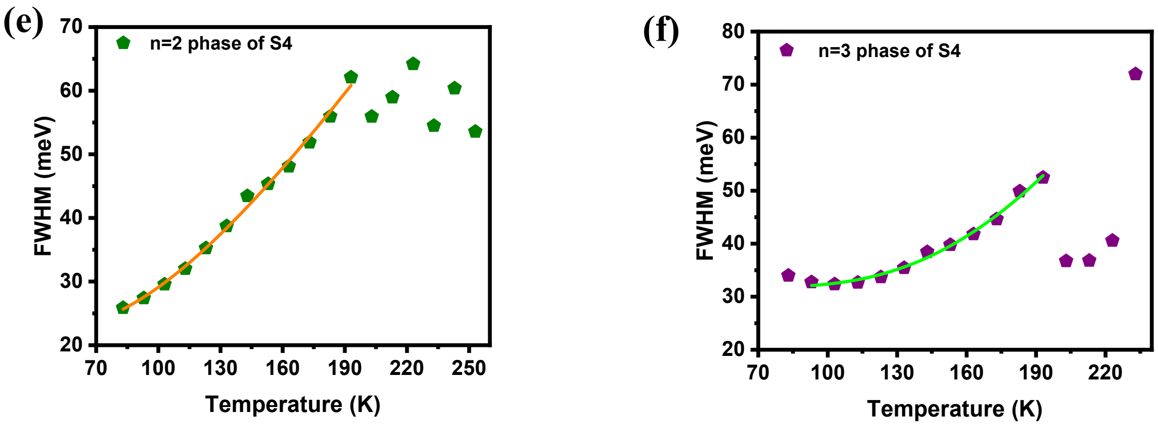

Fig. S9 Temperature-dependent full width at half maximum (FWHM) of the PL peaks for different phases of samples S2, S3 and S4. The solid lines represent the fitting results using eqn (8).

Table S4 The parameters estimated from fitting of experimental data shown in Fig. S9 using eqn (8).

Sample	Phase	Γ_0 (meV)	γ_{LO} (meV)	E_{LO} (meV)
S2	**n=2**	12.1 ± 0.4	33 ± 2	13.4 ± 0.2
	n=3	19.8 ± 0.4	157 ± 12	42 ± 1
	n=4	23.3 ± 0.6	108 ± 6	30.4 ± 0.8
S3	**n=2**	15.4 ± 0.4	153 ± 3	32.4 ± 0.3
	n=3	25.6 ± 0.4	843 ± 33	67 ± 1
	n=4	18.9 ± 0.8	493 ± 15	53.6 ± 0.9
S4	**n=2**	22.1± 0.6	164 ± 4	27.5 ± 0.3
	n=3	31.7 ± 0.3	845 ± 25	61.7± 0.5
	n=4	35.7 ± 0.9	695 ± 55	53 ± 1